Modeling the Bistability of An AlGaAs/GaAs Double-Barrier Resonant Tunneling Diode
By: Ezri Adelsbach

1. Abstract

This paper examines AlGaAs/GaAs double barrier resonant tunneling structures, specifically a model for their bistability range. The model used in this paper is based on a 1988 paper by F.W. Sheard and G.A. Tombs[1], which we modified by normalizing each barrier separately to determine each barrier's transmission coefficient. This model was then tested against experimental data from a similar resonant tunneling diode found in a paper by Fisher et al.[2], where a 45% error was found. This was attributed to the lack of inclusion of resonance as a variable for transmission coefficients, along with an oversimplification of the resonant tunneling diode's structure.

2. Introduction

Although essential to many fields, including cryptography, obtaining truly random numbers is difficult[2]. True randomness is when the output cannot be predicted given the initial conditions, internal structures, and history of past results[2]. True randomness can be obtained in many ways, including noise from instruments, chaotic systems, and quantum tunneling. Quantum phenomena, like tunneling, are especially appealing due to the intrinsic uncertainty that defines the phenomena[3]. Quantum tunneling is a characteristic that describes how particles can cross through energy barriers traditionally deemed to be impossible due to the laws of classical mechanics seen in Figure 1. Particles accomplish this because of their ability to exhibit wave-like and particle-like properties, and this occurs on a probabilistic basis[4]. Two of the largest factors that affect the probability of quantum tunneling are the thickness of the energy barrier and the amount of initial energy.

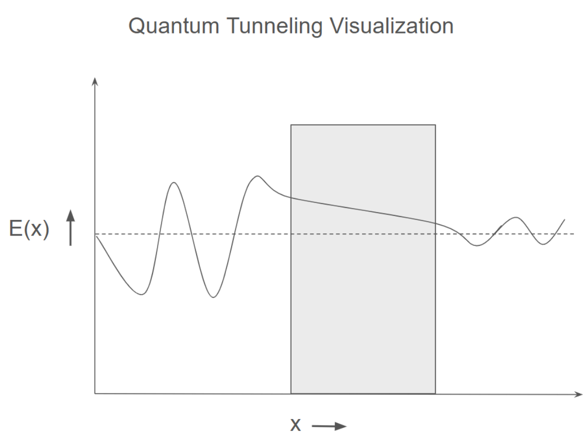

Figure 1: Visualization of a particle's energy when tunneling through a barrier. Notice that the energy stays the same, but the amplitude lowers after tunneling.

Resistance tunneling diodes(RTDs) consist of an emitter plate, two barriers that offset a quantum well, and a collector plate[5]. In this diode, electrons can tunnel through the well with the highest probability when the electron energy after tunneling matches a discrete energy level within the quantum well[3]. When exceeding this amount of energy, because the electrons are no longer tunneling to a discrete energy level, they have a decreased probability of tunneling beyond the barrier[3]. The discrepancy where voltage increases but the total flow of electrons decreases is called the negative differential resistance. This creates a peak where the total flow of electrons, current, will be highest for a specific voltage—this peak on the grey line at 0.25V in Figure 2.

Instead of using a voltage sweep, a current sweep can be applied to an RTD. When current increases, voltage increases in a positive relationship. Between the peak current discussed in the previous section and the soon-to-be-mentioned current intersection point, there is a massive jump in voltage. This massive increase in voltage is due to a change in resistance, going from a low resistance to a higher one[3]. This jump can be seen in Figure 2 when following the red line at seven mA.

When amperage decreases after the current sweep, the resistance does not decrease from the state before the current starts decreasing. This means that once the current is high enough for the resistance to increase, the resistance stays heightened even while amperage and voltage decrease[3]. The intersection of the Voltage and Current (V/I) graph of the negative differential resistance section for the voltage sweep and the high resistance but decreasing amperage line is the point at which the jump in resistance starts. The intersection can be seen in Figure 2 at 0.635V and 0.1 mA.

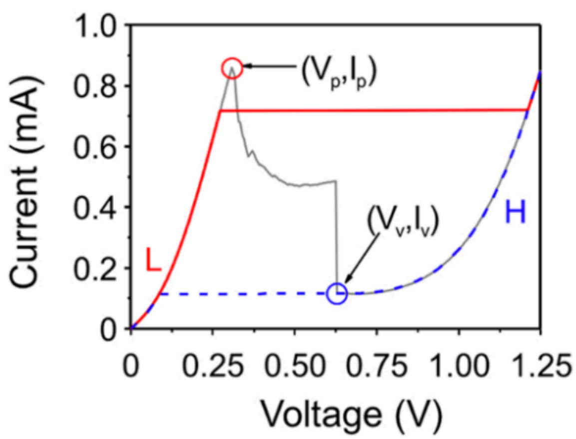

Figure 2: Current/Voltage relationship graph. The grey line represents the relationship during a voltage sweep. The red line represents the relationship during a current sweep with increasing current, and the blue line represents the voltage path when lowering current after RTD has jumped to the higher voltage. [4, Figure 1b]

This paper aims to analyze a model of this phenomenon for a common AlGaAs/GaAs RTD and determine the range in which the RTD's bistability is expressed. Therefore, this paper will model the flow of electrons through the RTD. Then, we will compare the results to experimental data written by Fisher et al. to determine the model's viability.

3 Characterization of the Resonant Tunneling Diode Used

3.1 Dimensions

To test the model, we needed to determine the dimensions of the RTD being used in this experiment. We modeled a simplified version of the RTD used in the Fisher et al. experimental paper. The RTD modeled was an $Al_xGa_{1-x}As/GaAs$ double barrier resonant tunneling heterostructure[2]. The collector, emitter, and quantum well were made from Gallium Arsenide, with the barriers made from Aluminum Gallium Arsenide that have an x ratio of 0.33. The barrier widths were asymmetrical, at 12 nm for the first barrier and 8 nm for the second barrier[2]. The collector and emitter plates were approximated for this model to be 55 nm of normal Gallium Arsenide. The barrier height of the Aluminum Gallium Arsenide can is approximated to be 2.164 electron volts[6].

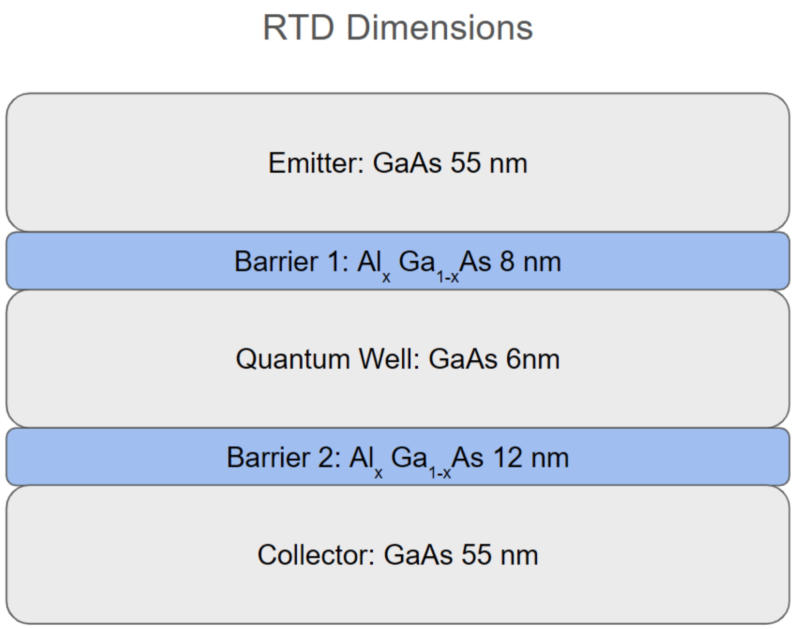

Figure 3: Schematic of the dimensions of RTD used for the theoretical model

3.2 Energy Structure Under Voltage Bias

The structure's potential energy changes under a voltage bias, allowing tunneling to occur[7]. When a voltage is applied to the RTD, the emitter side of the RTD rises in proportion to that voltage applied, while the collector side of the RTD does not increase in potential[1]. What differs from what may be expected is within the quantum well. Instead of the potential being exactly one-half of the voltage, we must account for voltage buildup within the well, denoted by the eϕ[1]. Additionally, eϕ was the average energy level within the well[1]; then, we straightened the entirety of the quantum well to have the same energy value of eϕ as seen in Figure 4. This approximation to create well with a constant potential helped simplify calculations found later.

For this paper, E_F was the fermi energy of the collector and emitter plates. Because they are made out of the same material, the two plates will have the same fermi energy[5]. V was the voltage applied to the system, and b_h was the potential of either barrier. Because the barriers were made out of the same material, they have the same potential[6].

$$V(x) = \begin{cases} E_F + eV & \text{emmitor} & -a \geq x \geq 0 \\ b_h + eV & \text{barrier 1} & 0 \geq x \geq b \\ e\phi & \text{quantum well} & b > x > c \\ b_h & \text{barrier 2} & c \geq x \geq c + b \\ E_F & \text{collector} & c + b > x > d \end{cases}$$

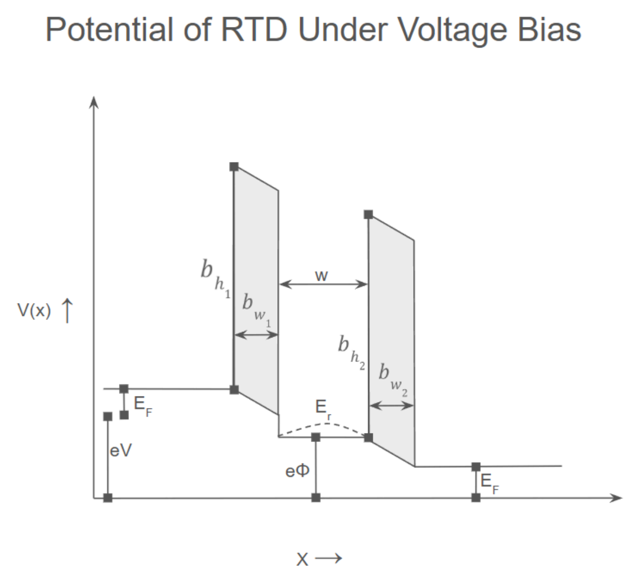

Figure 4: Diagram of RTD Potential

3.3 Wave Numbers and Wave Functions

Because of the differing potentials in the RTD, there were several different wave numbers depending on the place in the RTD. The wave functions were split into five different values. The first is k_{em}, which was the wave number for the emitter plate. κ_0 was the wave number within the first barrier. k_{qw} was the wave number within the quantum well. κ_1 was the wave number within the second barrier. Finally, k_{co} was the wave number within the collector. $b_{h_{1,2}}$ were the barrier heights combined with the effect caused by the voltage bias. The barrier heights were assumed to be constant, as seen in Figure 5.

$$k = \frac{\sqrt{2mE}}{\hbar} \text{ [5]}$$

$$k_{em} = \frac{\sqrt{2m(E_F + eV)}}{\hbar}$$

$$\kappa_0 = \frac{\sqrt{2m(b_{h_1} - (E_F + eV)}}{\hbar}$$

$$k_{qw} = \frac{\sqrt{2m(\,e\phi)}}{\hbar}$$

$$\kappa_1 = \frac{\sqrt{2m(b_{h_2} - (\,e\phi))}}{\hbar}$$

$$k_{co} = \frac{\sqrt{2mE_F}}{\hbar}$$

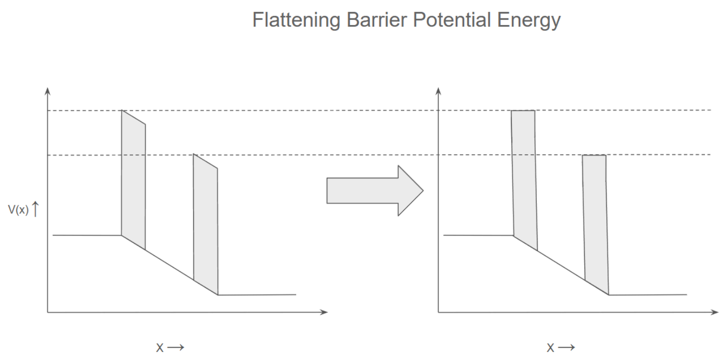

Figure 5: Potential barrier made constant for a more simple model

The time-dependent wave function was fairly standard. Because the particle was quasi-bound within the well, trig functions were used[5].

$$\psi(x) = \begin{cases} Ae^{ik_{em}x} + Be^{-ik_{em}x} & x \le 0 \\ Ce^{\kappa_0 x} + De^{-\kappa_0 x} & 0 \le x \le b_{w_1} \\ Ecos(k_{qw}x) + Fsin(k_{qw}x) & b < x < c \\ Ge^{\kappa_1 x} + He^{-\kappa_1 x} & c \le x \le c + b_{w_2} \\ Ie^{ik_{co}x} + Je^{-ik_{co}x} & c + b_{w_2} < x < d \end{cases}$$

3.4 Effective Mass

To determine the characteristics of the RTD, we needed to understand how electrons interact within the system. One measure that was considered was the electrons' effective mass. The effective mass was used over the free electron mass because the material's crystal lattice affects how the electrons react to forces enacted upon them[8].

Because the effective mass of an electron depends on the material's properties, the effective mass of the electron will depend on the material. The heterostructure is made up of two major materials, and to determine the characteristics of the electron through the entire system, we need to take a weighted average. The effective masses of Aluminum Gallium Arsenide and Gallium Arsenide are $(0.063 + 0.083x)\ m_e$ [9] (given $0<x<0.45$) and $0.063\ m_e$[10], respectively.

Determining the constant to multiply the electron mass required one more step for AlGaAs compared to GaAs, as it depended on the ratio of the different atoms in the material. The RTD we were studying had an x ratio of 0.33, so the effective mass of our AlGaAS was 0.09039 m_e. Given that the free electron mass was 9.10938×10^{-31}kg, m_s^* was the effective mass of the entire heterostructure, m_b^* was the effective mass of the barriers(AlGaAs), and m_w^* was the effective mass of the collector and emitter plates(GaAs), l_1 was the combined width in nm for the emitter, collector, and quantum well, while l_2 was the combined width of the of two barriers, the effective mass calculations for RTD would be:

$$m_s^* = \frac{l_1 m_w^* + l_2 m_b^*}{l_1 + l_2}$$

$$m_s^* = \frac{(50 + 5+6+5+50)\times 0.09039 + (12 + 8) \times 0.063}{50 + 5+6+5+50+12 + 8} \times 9.10938 \times 10^{-31} = 7.86704811 \times 10^{-32}\, kg$$

$$m_b^* = 0.09039 \times 9.10938 \times 10^{-31} = 6.049702 \times 10^{-32} = 8.2339685 \times 10^{-32}\, kg$$

$$m_w^* = 0.063 \times 9.10938 \times 10^{-31} = 6.049702 \times 10^{-32} = 5.73891 \times 10^{-32}\, kg$$

3.5 Resonating Energy Levels:

Another important characteristic of the RTD was its resonating energy levels, which were determined by the energy levels within the quantum well. We were looking at the first discrete energy level because it would be the first level that electrons tunnel into during a current or voltage sweep. Before any voltage was applied, the energy in the emitter plate was not high enough to even tunnel into the first level. So, when energy was added to the system, the first energy level reached would be the lowest. This lowest energy level, in our case, is the first energy level. Then, we can simply determine the height of the resonating energy level:

$$E_n = \frac{n^2 \hbar^2 \pi^2}{2mL^2} \text{ [5]}$$

$$E_r = \frac{1^2 \hbar^2 \pi^2}{2mL^2} = \frac{(1.05457 \times 10^{-34})^2 \pi^2}{0.067 \times 9.10938 \times 10^{-31} \times (6 \times 10^{-9})^2} = 2.497776 \times 10^{-20} J = 0.15589892241\, eV$$

3.6 Fermi Energy Level

The Fermi level, or Fermi energy, is also needed to determine the bistability of the RTD. Fermi energy is the energy level filled by the valence electrons at absolute zero [5]. This was needed for the emitter and collector plates. Furthermore, it was important to take into account the Fermi energy level because these levels will change the proportionality of the emitter plate and the initial barrier. Because the Fermi level depended on the electron configuration of the material, and the collector and emitter plates were made out of the same material, the two plates would have the same Fermi level. Given that we were looking at the Fermi energy of GaAs, N was the number of electrons in the material, V was the volume of material, and GaAs had a density of $5.31 \frac{g}{cm^3}$ and an atomic mass of $144.645 \frac{g}{mol}$, we solved for E_F, or the Fermi energy:

$$E_F = \frac{\hbar^2}{2m_w^*}\left(\frac{3\pi^2 N}{V}\right)^{\frac{2}{3}} \text{ [5]}$$

$$E_F = \frac{(1.0545718\times10^{-34})^2}{2\times5.73891\times10^{-32}}\left(\frac{3\pi^2 N}{V}\right)^{\frac{2}{3}}$$

$$\frac{N}{V} = \frac{density}{atomic\ mass} \times avogadro's\ number \text{ [5]}$$

$$\frac{N}{V} = \frac{5.31\frac{g}{cm^3}}{144.645\frac{g}{mol}} \times 6.023\times10^{23} = 2.211077466\times10^{22}$$

$$E_F = \frac{(1.0545718\times10^{-34})^2}{2\times0.063\times9.10938\times10^{-31}}(3\pi^2\times2.211077466\times10^{22})^{\frac{2}{3}} = 7.305\times10^{-22}J = 0.0045594226eV$$

3.7 Relative Permittivity

Another important factor in determining bistability was the relative permittivity of the different materials. The relative permittivity of a material is how much the material can polarize a material subject to an electric field[11]. A constant that would be used later was the permittivity in a vacuum: $\epsilon_0 = 8.85 \times 10^{-12}$. In order to determine this constant for the entire system, a weighted average was used. Given that the relative permittivity of Aluminum Gallium Arsenide and Gallium Arsenide were 11.9628 and 12.35, respectively, ϵ_w was the relative permittivity of the collector, emitter, and quantum well, ϵ_b was the relative permittivity of the barriers, and ϵ_r was the relative permittivity of the entire structure, we determined:

$$\epsilon_w = 12.35$$

$$\epsilon_b = 11.9628$$

$$\epsilon_r = \frac{l_1\epsilon_1 + l_2\epsilon_2}{l_1 + l_2}$$

$$\epsilon_r = \frac{(50+5+6+5+50)\times11.9628 + (12+8)\times12.35}{50+5+6+5+50+12+8} \approx 12.01974118$$

3.8 Determining Threshold Voltage

One characteristic explicitly described in the F.W. Sheard and G.A. Tombs paper is the threshold voltage. This voltage is applied to the structure where the onset of the tunneling begins [1]. Given V_{th} is the threshold voltage:

$$V_{th} = 2\frac{(E_r - E_F)}{e} \text{ [1]}$$

$$V_{th} = \frac{2(0.15728\,eV - 0.0045594226eV)}{e} = 0.3054411548\,V$$

4 Potential within Quantum Well and Transmission Coefficient Calculations
4.1 Calculating The Potential Within the Quantum Well

One problem when determining $e\phi$ was that the value changes depending on the voltage bias that is applied. To simplify calculations, we assumed voltage bias to be constant at the voltage threshold: $V_{th} \approx 0.3V$. This simplification allowed us to determine the charge buildup within the well experimentally. The T. A. Fisher et al. paper states that under a 0.3 Voltage bias, the charge buildup within the well is 0.0095 eV[2]. With this information, we can solve for $e\phi$, as it is half of the voltage bias plus the charge buildup within the well:

$e\phi = \frac{e}{2}V + \frac{1}{2}C$, where C is the charge buildup within the well:

$e\phi = 0.162$ eV

4.2 Barrier Isolation and Normalization

To examine each of the two different transmission coefficients(for the two barriers), the barriers were split up and looked at in isolation. For simplicity, we adjusted the potentials for all parts equally for either structure so that the point beyond the barrier(the quantum well for the first barrier and the collector plate for the second barrier) was at V(x) = 0. For the 1st barrier, we assumed the quantum well to be constantly at eϕ, so we subtracted that value from the entirety of the structure. This left the quantum well at no potential energy, as seen in Figure 6a. For the second barrier, we subtracted the fermi energy found on the collector plate; this left the normalized potential energy found in Figure 6b.

4.3 Barrier Heights Under Voltage Bias

To find the transmission coefficients, we needed to find the relative barrier heights under a voltage bias. We used the barrier isolation and normalization potentials found in 4.2. The relative barrier heights are denoted $b_{h_{1,2}}$ for the first and second barriers in Figures 6a and 6b.

$$b_{h_1} = b_h + eV - e\phi$$

$$b_{h_1} = 2.168 + 0.3054411548 - 0.162 = 2.31eV$$

$$b_{h_2} = b_h + e\phi - E_F$$

$$b_{h_2} = 2.168 + 0.162 - 0.0045594226eV = 2.33\ eV$$

Figure 6: Barrier Isolation within the RTD:

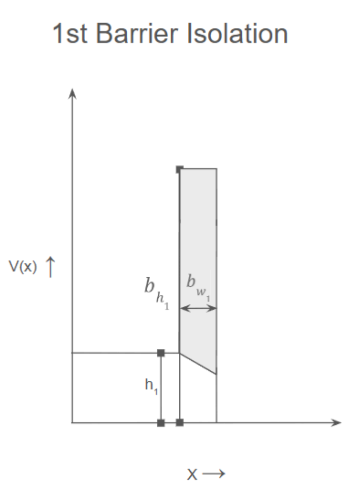

Figure 6a: 1st barrier adjusted so that the quantum well is at 0 potential energy

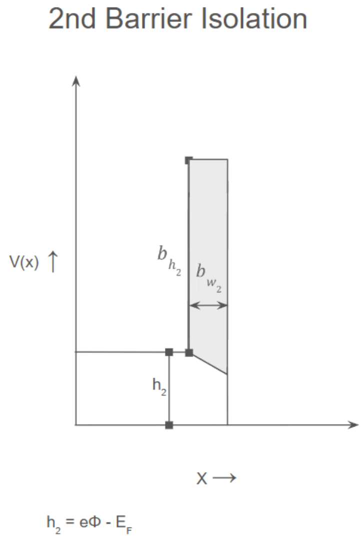

Figure 6b: 2nd barrier adjusted so that the collector plate is at 0 potential energy

4.4 WKB Approximation

The transmission coefficients were another necessary factor in determining this RTD's bistability window. The transmission coefficients were solved with a WKB approximation. The WKB method was a technique for obtaining approximate solutions to the time-independent Schrodinger equation in one dimension[12]. These WKB approximations are best used in cases where potentials do not vary greatly[12]. Due to our previous simplification of the RTD, our barriers were constants, meaning that WKB approximations were a viable option.

Given V(x) was the energy potential of the barrier, E was the energy of the particle, ψ was the time-independent Schrodinger Equation, and m was the effective mass of the particle in the barrier, the general solution for the WKB approximation when determining transmission coefficients was:

$T = e^{-2y}$ [12]

$y = \frac{1}{\hbar}\int_a^b |p(x)|dx$, given:

$$\frac{d^2\psi}{dx^2} = -\frac{p(x)^2}{\hbar^2}\psi$$

$$p(x) = \sqrt{2m[V(x) - E]}$$

4.5.1 Emmiter Transmission Coefficient

When calculating the transmission coefficient for the first barrier, we used the normalized and isolated potentials. Additionally, we used a constant voltage, the previously mentioned threshold voltage, to simplify the calculation. Finally, the variable m was the effective mass of the barrier and b_{w_1} its width.

$$\frac{d^2\psi}{dx^2} = -\frac{p(x)^2}{\hbar^2}\psi$$

$$\frac{d^2\psi}{dx^2} = -\frac{2m(b_{h_1} - (eV+E_F - e\phi))}{\hbar^2}\psi$$

$$p(x) = \sqrt{2m(b_{h_1} - (eV + E_F - e\phi))}$$

$$y = \frac{1}{\hbar}\int_0^{b_{w_1}} \left|\sqrt{2m(b_{h_1} - (eV + E_F - e\phi))}\right| dx$$

$$y = [\frac{x}{\hbar}\left|\sqrt{2m(b_{h_1} - (eV + E_F - e\phi))}\right|]|_0^b$$

$$y = \frac{b_{w_1}}{\hbar}\left|\sqrt{2m(b_{h_1} - (eV + E_F - e\phi))}\right|$$

$$T_e = e^{-2y} = e^{-2\frac{b_{w_1}}{\hbar}\left|\sqrt{2m(b_{h_1} - (eV+E_F - e\phi))}\right|}$$

$$T_e = e^{-2\frac{12\times10^{-9}}{6.582119569\times10^{-16}}\left|\sqrt{2\times8.2339685\times10^{-32}(2.31eV - (0.3054411548eV + 0.0045594226eV - 0.1622))}\right|}$$

$$T_e = e^{-2.17\times10^{-8}}$$

4.5.1 Collector Transmission Coefficient

Because of the charge buildup within the well, the difference in barrier widths, and the fermi energy of the collector and emitter plates, the second barrier's transmission coefficient was different compared to the first barrier. C was the x coordinate found previously when describing the potential of the system and the wave function, and m was the effective mass of the barrier.

$$\frac{d^2\psi}{dx^2} = -\frac{p(x)^2}{\hbar^2}\psi$$

$$\frac{d^2\psi}{dx^2} = -\frac{2m(b_{h_2} - (e\phi - E_F))}{\hbar^2}\psi$$

$$p(x) = \sqrt{2m(b_{h_2} - (e\phi - E_F))}$$

$$y = \frac{1}{\hbar}\int_c^{c+b_{w_2}} \left|\sqrt{2m(b_{h_2} - (e\phi - E_F))}\right| dx$$

$$y = [\frac{x}{\hbar}\sqrt{2m(b_{h_2} - (e\phi - E_F))}\,]|_c^{c+b_{w_2}}$$

$$y = \frac{b_{w_2}}{\hbar}\left|\sqrt{2m(b_{h_2} - (e\phi - E_F)}\right|$$

$$T_c = e^{-2y} = e^{-2\frac{b_{w_2}}{\hbar}\left|\sqrt{2m(b_{h_2} -(e\phi - E_F))}\right|}$$

$$T_c = e^{-2y} = e^{-2\frac{b_{w_2}}{\hbar}\left|\sqrt{2m(b_{h_2} -(e\phi - E_F))}\right|}$$

$$T_c = e^{-2y} = e^{-2\frac{8\times10^{-9}}{6.582119569\times10^{-16}}\left|\sqrt{2\times8.2339685\times 10^{-32}(2.33\ eV -(0.16222\ eV - 0.0045594226))}\right|}$$

$$T_c = e^{-2\frac{8\times10^{-9}}{6.582119569\times10^{-16}}\left|4.988\times10^{-16}\right|}$$

$$T_c = e^{-8.327\times10^{-9}}$$

5 Results, Analysis, and Discussions

5.1 Feedback Parameter

The feedback parameter controls the intrinsic bistability range α, as found in the F.W. Sheard and G.A. Tombs paper[1].

$$\alpha = \frac{2b+w+2\lambda}{\alpha_0}\frac{T_e}{T_e+T_c}[1]$$

$$\alpha_0 = \frac{4\epsilon_r\epsilon_0\hbar^2}{m_s^* e^2}\ [1]$$

$$\alpha_0 = \frac{4\times12.01974118\times 8.85\times10^{-12}\times(6.582119569\times10^{-16})^2}{7.86704811\times10^{-32}\times(1)^2} = 2.34\times10^{-9}$$

$$\frac{T_e}{T_e+T_c} \approx \frac{1}{2}$$

$$\alpha = \frac{2(2\times10^{-9})+(3\times10^{-9})+2\lambda}{2.34\times10^{-9}}\frac{1}{2}$$

We used the de Broglie wavelength equation to solve for wavelength, where h was Planck's constant and p was the particle's momentum.

$$\lambda = \frac{h}{p}\ [5]$$

$$p = \sqrt{2m_s^* E}$$

$$p = \sqrt{2m_s^*(E_F + eV)}$$

$$p = \sqrt{2\times7.86704811\times10^{-32}(0.004559 + 0.30544)}$$

$$\lambda = 2.2085\times10^{-16}\ \mathrm{m}$$

$$\alpha = \frac{(12\times10^{-9})+(8\times10^{-9})+(6\times10^{-9})+2\times2.2085\times10^{-16}}{2.34\times10^{-9}}\frac{1}{2}$$

$$\alpha = 5.6$$

3.2 Bistability Window

The initial point of bistability was the lowest voltage bias, where the resonating tunneling diode could be found with either of the two resistances. The beginning of the bistability range began at $2E_r$ [5]:

$$2 \times E_r = 0.3117978\,V$$

Furthermore, the window of this bistability, or the range of voltages where bistability can occur, was found as be equal to $2\alpha E_F$ [1]:

$$2\alpha E_F = 2 \times 5.6 \times 0.004559$$

$$2\alpha E_F = 0.05106\,V$$

To find the end of the bistable voltage, we could simply add the initial point of bistability to the bistable window:

$$End\ of\ Bistability = 2E_r + 2\alpha E_F$$

$$End\ of\ Bistability = 0.3628578\,V$$

3.3 Comparison to Experimental Data:

In the 1994 paper by Fisher et al., they tested an RTD made of the same material with the same dimensions. In this experiment, they determined the first peak between positive differential resistance and negative differential resistance through a sweep in voltage bias. This point, as mentioned earlier, is the end of the bistable window. The values given were 0.66V[2]. When comparing the experimental values of 0. 36V to the theoretical ones, there was a 45% error.

3.4 Error Analysis

The error can be divided into two major categories. The first category is due to the simplification of the RTD model in Figure 5. This simplification completely overlooked the prewell layer of Indium Gallium Arsenide, which may affect the transmission coefficients. The emitter and collector plates were also doped n^+, which the simplified model ignored. This would affect Fermi's energy and, along with the force, act upon the electrons within the structure.

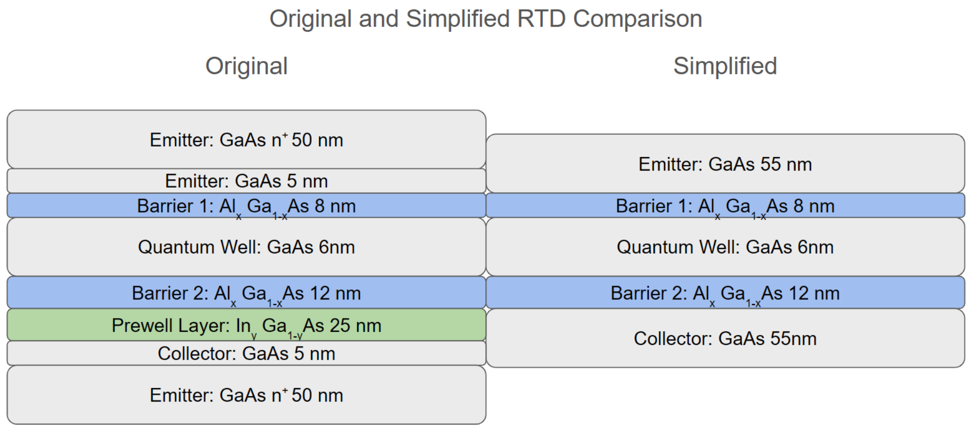

Figure 5: The simplified model completely ignores the Indium Gallium Arsenide layer and assumes the collector and emitter to be non-doped Gallium Arsenide

The second category of error that was important was the WKB approximations used in determining the transmission coefficients. These WKB approximations did not consider that when tunneling into a double barrier structure at a resonating energy level, there was a higher transmission coefficient. Modifying the method of finding the transmission coefficients so that resonance is taken into account would create a more accurate model.

4. Conclusion

In this paper, we modeled the bistability window of an AlGaAs/GaAs resonant tunneling diode using its dimensions, material makeup, and known charge buildup at threshold voltage. The model's basis came from a paper by Sheard and Tombs, and WKB approximations were used to determine the transmission coefficients.

This bistability window was compromised of an initial point of bistability, or at what voltage the bistability begins, and the bistability range, which is the voltage range for this bistability. With this information, we could easily determine the point at which the bistability ends.

The bistability initial and end points were then compared to an experimental paper by Fisher et. In a paper written by Fisher et al., they were focused on determining the charge buildup within a double barrier structure, but they also analyzed the current-voltage relationship under a voltage sweep. In this voltage sweep, the peak between positive differential resistance and negative differential resistance is the point at which the bistability window ends. By being able to experimentally determine the point at which bistability ends, we can compare the results to what the theoretical model yields. The theoretical model had a 45% error compared to the experimental paper. This error could be attributed to the WKB approximations and the simplicity of the model.

Because of the high error, the model certainly needs to incorporate more factors to increase accuracy. Nonetheless, creating this theoretical model is important in understanding how the bistability of RTDs can be used to generate random numbers.

Bibliography

[1]
F. W. Sheard and G. A. Toombs, “Space-charge buildup and bistability in resonant-tunneling double-barrier structures,” Applied Physics Letters, vol. 52, no. 15, pp. 1228–1230, Apr. 1988, doi: 10.1063/1.99165.

[2]
T. A. Fisher *et al.*, “Use of a narrow-gap prewell for the optical study of charge buildup and the Fermi-energy edge singularity in a double-barrier resonant-tunneling structure,” *Phys. Rev. B*, vol. 50, no. 24, pp. 18469–18478, Dec. 1994, doi: 10.1103/PhysRevB.50.18469.

[3]
F. Yu, L. Li, Q. Tang, S. Cai, Y. Song, and Q. Xu, “A Survey on True Random Number Generators Based on Chaos,” *Discrete Dynamics in Nature and Society*, vol. 2019, pp. 1–10, Dec. 2019, doi: 10.1155/2019/2545123.

[4]
R. Bernardo-Gavito *et al.*, “Extracting random numbers from quantum tunnelling through a single diode,” *Sci Rep*, vol. 7, no. 1, p. 17879, Dec. 2017, doi: 10.1038/s41598-017-18161-9.

[5]
J. S. Townsend, *Quantum physics: a fundamental approach to modern physics*. Sausalito, California: University Science Books, 2010.

[6]
N. Govind and S. J. Dhoble, *The Fundamentals and Applications of Light-Emitting Diodes*. Elsevier, 2020. doi: 10.1016/C2019-0-00273-7.

[7]
D. Goldhaber-Gordon, M. S. Montemerlo, J. C. Love, G. J. Opiteck, and J. C. Ellenbogen, “Overview of nanoelectronic devices,” *Proc. IEEE*, vol. 85, no. 4, pp. 521–540, Apr. 1997, doi: 10.1109/5.573739.

[8]
M. Tulakder, “Effective Mass,” [Online]. Available: https://anis.buet.ac.bd/Teaching/properties_of_materials/Lecture17.pdf

[9]
“Basic Parameters of AlGaAs at 300k.” Ioffe Institute. [Online]. Available: https://www.ioffe.ru/SVA/NSM/Semicond/AlGaAs/basic.html

[10]
“Basic Parameters of GaAs at 300k.” Ioffe Institute. [Online]. Available: https://www.ioffe.ru/SVA/NSM/Semicond/GaAs/basic.html

[11]
R. Dorey, *Ceramic thick films for MEMS and microdevices*. in Micro & Nano Technologies Series. Oxford: William Andrew, 2012.

[12]
D. J. Griffiths and D. F. Schroeter, *Introduction to Quantum Mechanics*, 3rd ed. Cambridge University Press, 2018. doi: 10.1017/9781316995433.